Volume and Activity Quantitation with Iodine-123 SPECT

David R. Gilland, Ronald J. Jaszczak, Timothy G. Turkington, Kim L. Greer and R. Edward Coleman

Department of Radiology, Duke University Medical Center, Durham, North Carolina

The goals of this study were to investigate the effect of septal penetration on ^{123}I SPECT activity quantitation using low-energy, high-resolution collimators, and to evaluate a semi-automatic method for measuring volume and activity of ^{123}I distribution with SPECT. **Methods:** Data were acquired from experimental phantoms containing spheres filled with a high-purity ^{123}I solution. The penetration study compared the reconstructed activity of a 3.4-cm diameter sphere with and without the presence of surrounding activity. In the study of volume and activity quantitation, three different size spheres (diameters of 1.8 cm, 2.8 cm and 3.4 cm) were imaged in three different sphere-to-background (S:B) ^{123}I concentration ratios (2.5, 5 and 10) with low-energy collimators. The filtered backprojection reconstruction method was used with compensation for scatter, attenuation and detector response. Volume and activity measurements were obtained from the SPECT image using a semiautomatic gradient technique which estimates the location of the sphere/boundary in three dimensions. **Results:** With the low-energy collimator, there was only a small (<2%) increase in the measured activity of the sphere when surrounding activity was present. The measured volume for the two largest spheres was within 5% of the true volume for all S:B ratios. The activity measurement of these spheres was consistently underestimated by 20%–25% but suggested that the accuracy could be improved with calibration. For the smallest sphere, the volume was grossly overestimated and only at the 10 S:B ratio was the activity measured reasonably accurately (<20%). **Conclusions:** The low-energy collimators used in this study are suitable for quantitative ^{123}I SPECT. Accurate SPECT volume and activity quantitation of ^{123}I distribution can be achieved by semiautomatic means at clinical count densities for objects as small as 2.8 cm in diameter and reasonable activity quantitation is possible for smaller objects with an S:B ratio of at least 10.

Key Words: iodine-123; SPECT; activity quantitation; volume quantitation; septal penetration

J Nucl Med 1994; 35:1707–1713

Accurate volume and activity quantitation with SPECT can provide important information for radiolabeled monoclonal antibody (Mab) imaging and in dosimetry determination for cancer treatment. Volume information obtained with SPECT provides a means of monitoring changes in tumor growth. Knowledge of tumor activity can help in the design of strategies for improving the Mab uptake in tumors and along with tumor volume, can facilitate dose estimation to tumor and normal tissue. Accurate dose estimation and tumor volume can allow investigation into the relationship between tumor radiation dose and therapeutic response. The primary objective of this study, therefore, was to implement a method for measuring volume and activity with SPECT and evaluate its quantitative accuracy and precision. This study focused on ^{123}I, a radionuclide that is potentially important in Mab imaging, as well as in the treatment dosimetry for thyroid disease.

SPECT volume and activity measurement can be greatly affected by physical factors that include attenuation, scatter, detector response and septal penetration. Detector response effects in particular can be severe for small tumors and small tumor-to-normal uptake ratios. For tumors smaller than approximately twice the system FWHM, the reconstructed activity concentration decreases with tumor size (*1*). Whereas for large uptake ratios (>10) the total tumor activity for even these small tumors can be measured with reasonable accuracy with an ROI that loosely encompasses the tumor. For smaller uptake ratios the measured activity is greatly affected by the ROI size and how much normal tissue is included. In this case, some means of distinguishing between tumor and normal tissue must be employed.

Objective methods for distinguishing tumor from normal tissue in SPECT images have followed either the threshold or gradient approaches. An excellent review of these methods in the context of SPECT volume determination can be found in King et al. (*2*). With the threshold approach, voxels are considered part of the tumor if their intensity is greater than (hot tumors) or less than (cold tumors) a specified cut-off value. This value is often expressed as a percentage of the maximum intensity in the tumor region. The problem with the threshold methods is the same as with the loose ROI approach: large quantitative errors may be introduced when there is significant uptake in normal tissue. This is illustrated in the results of an experimental phantom study shown in Figure 1. The measured volume of a 21.5-

Received Nov. 29, 1993; revision accepted Apr. 7, 1994.
For correspondence and reprints contact: David R. Gilland, PhD, Dept. of Radiology, Box 3949, Duke University Medical Center, Durham NC 27710.

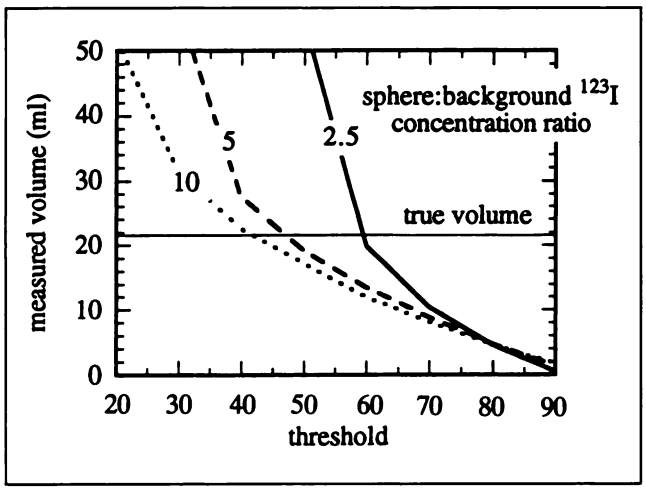

FIGURE 1. Measured volume as a function of selected threshold for three sphere-to-background ^{123}I concentration ratios.

ml, ^{123}I-filled sphere situated within a uniform background distribution of ^{123}I is plotted as a function of the specified threshold for 10, 5 and 2.5 sphere-to-background ^{123}I concentration ratios. The plot illustrates the sensitivity of the measured sphere volume to the chosen threshold and the fact that the threshold that gives the correct volume is highly dependent on the sphere-to-background ^{123}I concentration ratio.

In order to avoid the problems associated with threshold methods, this study employed a gradient approach for the ^{123}I SPECT volume and activity quantitation. Other investigators have demonstrated accurate SPECT volume determination with sophisticated gradient methods applied to simulated data (*3*). This study implemented a relatively simple and efficient technique, which is tailored for the tumor characteristics encountered in clinical Mab imaging, and evaluated the technique with experimental ^{123}I phantom data. A range of tumor size and tumor-to-normal uptake ratios were examined, and count densities were acquired that are representative of clinical Mab imaging. The reconstruction method compensated for physical factors that affect the measured SPECT data, including scatter, attenuation and detector response so that not only volume, but activity measures may also be obtained.

An additional concern with quantitative ^{123}I SPECT is the choice of collimator. The higher energy emissions of ^{123}I (2.6% between 248 keV and 540 keV and 0.21% between 624 and 785 keV (*4*)) can penetrate the septa of low-energy collimators and potentially affect quantitative accuracy. Contamination from other isotopes of iodine, including ^{124}I, ^{125}I and ^{126}I, during production of ^{123}I can similarly affect quantitative accuracy with low-energy collimators. Previous studies have compared low- and medium-energy collimators for ^{123}I imaging although not directly in terms of SPECT quantitation (*5–8*). Macey et al. (*5*) recommended medium-energy over low-energy collimators for SPECT quantitation of ^{123}I labeled Mabs although SPECT quantitation was not explicitly investigated. Interpretation of this previous work is complicated by the different methods of ^{123}I production used in these studies.

Past investigations have used ^{123}I generated either directly by the ^{124}Te (p, 2n) ^{123}I reaction, or indirectly by the ^{127}I (p, 5n) ^{123}Xe reaction. The latter method is known to result in less contamination from other iodine isotopes. For this study, however, the ^{123}I was produced indirectly by the ^{124}Xe (p, 2n) ^{123}Cs reaction (Nordion International, Inc., Vancouver, British Columbia, Canada) which results in less contamination from ^{124}I (<0.0001%), ^{125}I (<0.02%), and ^{126}I (<0.0001%) than either of the other methods. The secondary objective of this study was to evaluate the effect of penetration on quantitative SPECT with high purity ^{123}I and low-energy, high-resolution collimators.

MATERIALS AND METHODS

Iodine-123 Penetration with Low-Energy Collimators

The initial phantom study was aimed at evaluating the effect of septal penetration on ^{123}I SPECT quantitation with low-energy, high-resolution collimators. The study investigated the extent to which the measured activity in an ROI is affected by penetrating photons originating from surrounding activity.

Phantom. A 3.4-cm diameter sphere filled with ^{123}I solution at a concentration of approximately 0.17 MBq/ml was imaged with and without the presence of surrounding activity. This surrounding activity consisted of three additional spheres, each approximately 5.6 cm in diameter and filled with ^{123}I at the same 0.17-MBq/ml concentration. All spheres were located approximately in the same transaxial plane, and the center-to-center distances between the 3.4-cm diameter sphere and each of the three additional spheres were 11.5 cm, 12.6 cm and 15.8 cm (Fig. 2A). Thus, the distance between the 3.4-cm diameter sphere and the surrounding activity prohibited any cross-talk between the two regions by spatial resolution effects. Also, the phantom background contained only air which prohibited cross-talk by scatter effects.

Data Acquisition. All data in this investigation were acquired on a three-headed SPECT system (Trionix Research Laboratories, Inc., Twinsburg, OH). Two heads were mounted with low-energy, ultra-high resolution collimators (LEUR) and the third with a medium-energy collimator (MEDE). The LEUR collimators have a 35.7-mm hole length, a 0.16-mm septal thickness and a 1.38-mm effective hole diameter. The respective parameters for the MEDE collimator are 59.0 mm, 1.17 mm and 3.25 mm. The SPECT acquisitions consisted of 120 projection angles over 360° for a total scan time of 30 min. The radius of rotation from the detector crystal was 25 cm and the pixel size was 3.6 mm. The energy window was 15% in total width and centered on the 159-keV photopeak. In addition to the SPECT acquisitions, line-spread function and energy spectrum measurements were performed with both collimator types using a line source of ^{123}I.

Processing and Analysis. The data in this study were reconstructed by the filtered backprojection method using a ramp filter with one iteration Chang attenuation compensation (*9*). An attenuation map for the compensation method was constructed based on the known size and location of the spheres and the linear attenuation coefficient of 159-keV photons in water (0.147 cm^{-1}) (*10*). Before reconstruction, the data were filtered with a two-dimensional Hann filter with cut-off frequency equal to the Nyquist frequency (1.4 cycles/cm). This filter, providing a small

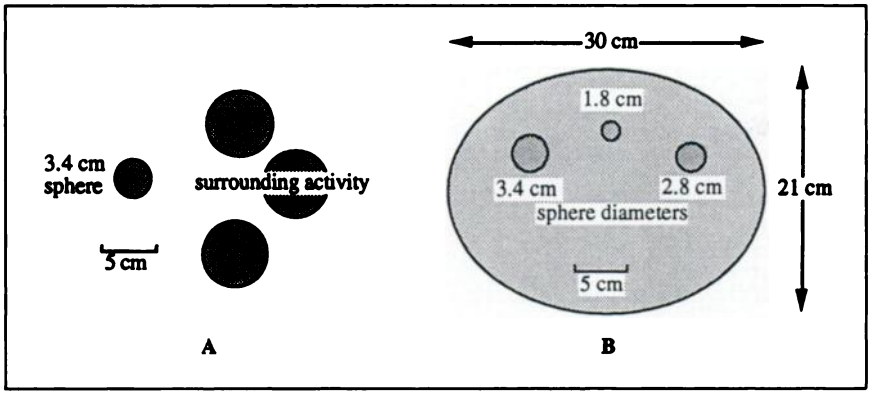

FIGURE 2. Cross-section diagrams of experimental phantoms. (A) ^{123}I penetration experiment. (B) ^{123}I volume and activity measurement.

degree of noise control, was adequate for the purposes of this study since spatial resolution was not an issue. The total activity of the 3.4-cm sphere was measured in the SPECT image by summing the counts within a loose three-dimensional ROI encompassing the sphere and dividing by the scan time (seconds) and the system sensitivity factor (counts per second per MBq). The sensitivity factor was determined for both the LEUR and the MEDE collimators using a point source of known activity. The ROI was manually drawn using an image display program developed within our laboratory and was large enough to completely contain the blurred sphere without overlapping the regions of the surrounding spheres.

The total sphere activity estimated from the SPECT image was compared to an independent planar measurement that excluded the effects of attenuation, scatter, detector response and penetration. A planar acquisition (30 min) was performed with a 3-ml syringe filled with a sample of the sphere solution. The total counts were extracted within an ROI that was just large enough to contain the blurred syringe. The estimate of the total sphere activity was then obtained by dividing the total syringe counts by the scan time and the system sensitivity factor, then multiplying by the sphere-to-syringe volume ratio. The sphere volume was measured accurately based on the mass difference between the empty and water-filled sphere.

Volume and Activity Measurement with Iodine-123 SPECT

The objective of this second phantom study was to evaluate the quantitative accuracy of volume and activity measurements of ^{123}I-filled spheres located in a uniform background distribution of ^{123}I. The SPECT reconstruction and processing methods compensated for the physical factors that affect the measured data. A semiautomatic technique was used to obtain the volume and activity measures from the SPECT images.

Phantom. Three spheres of diameters 1.8 cm, 2.8 cm and 3.4 cm (3.4 ml, 12.0 ml and 21.5 ml, respectively) were filled with ^{123}I solution at a concentration of approximately 0.044 MBq/ml and mounted inside an elliptical cylinder phantom, 30 cm × 22.5 cm in cross-section and 20 cm tall (Fig. 2B). The cylinder was filled with ^{123}I solution initially at a concentration of approximately 0.0044 MBq/ml, producing a sphere-to-background (S:B) ^{123}I concentration ratio of 10. Subsequently, ^{123}I was added to the background at two stages to produce S:B ratios of 5 and 2.5.

Data Acquisition. Two SPECT acquisitions were performed for each of the three S:B ratios using the SPECT system, collimators and acquisition parameters described in the penetration study. In addition to the photopeak energy window described previously, a secondary window (103–146 keV) was acquired for purposes of scatter compensation. As in the penetration study, a 30-min planar acquisition was performed with a 3-ml syringe filled with a sample of the spheres' ^{123}I solution in order to obtain an estimate of the true activity in the absence of attenuation, scatter, detector response and penetration effects.

Processing and Reconstruction. The acquired phantom data were compensated for scatter before reconstruction using a subtraction method (*11*). The k value for the compensation was 0.35 and was determined experimentally using line source data in the manner described by Jaszczak et al. (*11*). The scatter-compensated data were then filtered with a two-dimensional Metz filter (*12*) that was modified in the manner described in King et al. (*13*). The MTF in the filter formula was a Gaussian function with FWHM equal to 1.15 cm after discrete inverse Fourier Transform. This closely matched the FWHM of the measured line spread function with the LEUR collimator at a distance from the collimator equal to the radius of rotation. The P, S and X parameters in the filter formula (*13*) were 1.3, 0.152 and 50, respectively, and the units of the frequency variable were cm^{-1}. These parameters were selected to achieve a visually pleasing image in terms of the noise and resolution characteristics. The one-dimensional version of the filter is shown in Figure 3.

Data were reconstructed by the filtered backprojection method using a ramp filter and one iteration of Chang attenuation compensation. The attenuation map was constructed based on the known size and location of the phantom assuming a uniform linear

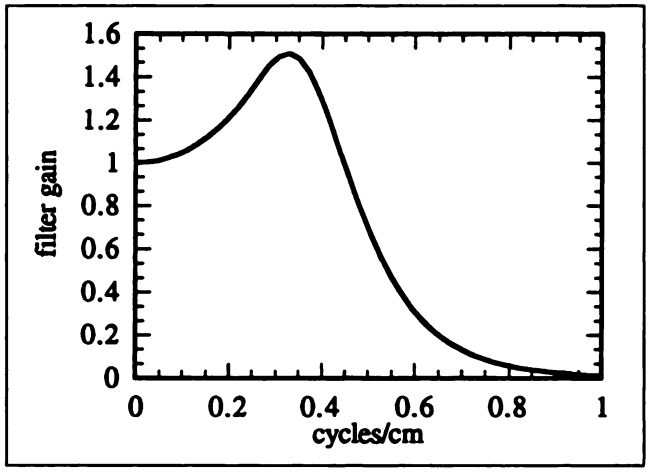

FIGURE 3. Metz filter.

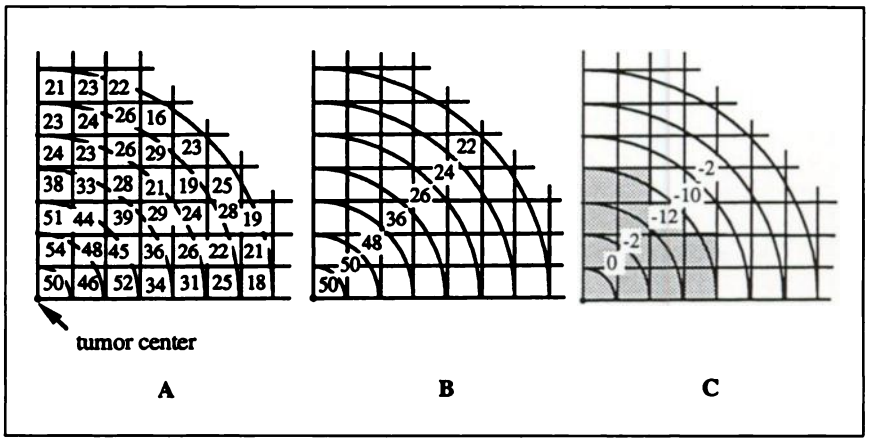

FIGURE 4. Two-dimensional example of tumor boundary determination. (A) Original image showing tumor center and shells. (B) Computed radial intensities. (C) Gradient of radial intensity. Shaded pixels are included within boundary.

attenuation coefficient of 0.147 cm^{-1}. A median filter with a 3 × 3 × 3 kernel was applied to the SPECT image to further reduce noise while preserving edges.

Volume and Activity Measurement. A new method was used to obtain the volume and activity measures from the SPECT image. Rather than thresholding based on voxel intensities, the method attempts to find the tumor boundary by examining the three-dimensional intensity gradient in the vicinity of the tumor. This method is tailored for hot tumors with hot centers and is semiautomatic in the sense that it only requires the operator to specify a loose ROI encompassing the tumor in the SPECT image. Generally, the SPECT image will contain multiple foci of increased uptake, and so the operator must specify for which of these the quantitative measurement is desired. This ROI must be broad enough to completely contain the tumor, and the tumor must be the most intense activity in the region. The loose ROI can be specified relatively quickly using three-dimensional image display methods.

Finding the three-dimensional boundary of the tumor and obtaining the volume and activity measurements are done in the following way. First, the three-dimensional location of the tumor center is estimated from the SPECT image in a way analogous to the center of gravity computation using the count rate distribution rather than the mass distribution. We have observed more satisfactory results in locating the tumor center when this calculation is performed only considering voxels that are greater than half the maximum intensity in the loose ROI. This better handles the situation in which the tumor is not centered in the loose ROI.

Intensity gradients are then computed starting from the estimated tumor center and moving radially outward in eight equally spaced directions corresponding to the octants of a three-dimensional coordinate space centered at the estimated tumor center. These eight radial gradients are computed by first averaging voxel intensities within one-voxel-thick shells within each octant and then applying a [−1 1] convolution kernel. Finally, the minimum is located for each of the eight gradients, and this defines the tumor boundary within that octant. This procedure for finding the tumor boundary is illustrated for the two-dimensional case in Figure 4. Tumor volume can then be computed by counting the number of voxels within the boundary and multiplying this number by the volume per voxel. Tumor activity can be computed from the SPECT image by summing the counts within the boundary and dividing this number by the scan time and the system sensitivity factor.

Analysis of Volume and Activity Measurements. The results of the volume and activity measurements are presented in terms of both the accuracy, or percent error in the mean of the sample measurements from the "truth":

$$\%\ \text{error} = \frac{\text{sample mean} - \text{"truth"}}{\text{"truth"}} \times 100,$$

and precision, or the percent s.d. of the sample measurements:

$$\%\ \text{s.d.} = \frac{\text{sample s.d.}}{\text{sample mean}} \times 100.$$

The "truth" for the volume measurement was obtained from the difference in mass measurements of the empty and water-filled spheres. For the activity measurement, the "truth" was obtained from the planar acquisition of a 3-ml syringe sample in the manner previously described. For the LEUR collimator, the two SPECT acquisitions and two camera heads per acquisition resulted in four sample measurements.

RESULTS

Iodine-123 Penetration with Low-Energy Collimators

The effects of ^{123}I penetration with the LEUR collimators can be seen in comparing the detected energy spectra with the LEUR and MEDE collimators shown in Figure 5. A larger number of photons are detected at energies above the primary photopeak energy with the LEUR collimator compared with the MEDE collimator. These are most likely the higher-energy emissions of ^{123}I that have penetrated the septa of the low-energy collimator and Compton scattered within the detector. The effects of penetration with the LEUR collimators are also observed in the line-spread functions in Figure 6 where broad tails are present in the LEUR case but not in the MEDE case. The magnitude of the tails is approximately 2% of the peak intensity near the peak and slowly decreases to approximately 0.5% at a distance of 30 pixels (10.8 cm) from the peak.

The effects of penetration on activity quantitation with LEUR collimators was found to be relatively small. The measured activity in the 3.4-cm diameter sphere was 3.27 MBq without and 3.33 MBq with the presence of the sur-

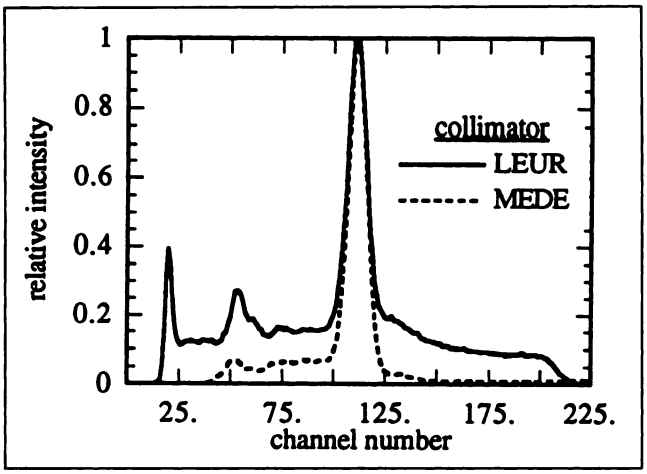

FIGURE 5. Detected ^{123}I energy spectra with low- and medium-energy collimators.

rounding activity for an increase of approximately 2%. With total counts in each of these measurements of approximately 750,000, the percent root mean squared uncertainty in this difference due to image noise is expected to be less than 1.0% (*14*). The true activity based on the planar acquisition of the syringe sample was 3.39 MBq. With the MEDE collimator, the measured activity was 3.23 MBq without and 3.20 MBq with surrounding activity. This difference is likely due to image noise.

Volume and Activity Measurement with Iodine-123 SPECT

The evaluation of volume and activity quantitation with ^{123}I focused on the LEUR collimator results since penetration did not substantially affect quantitation and because the LEUR collimator has better resolution with approximately equal sensitivity compared to the MEDE collimator. The results of the evaluation are presented in Table 1 for the three sphere sizes and three

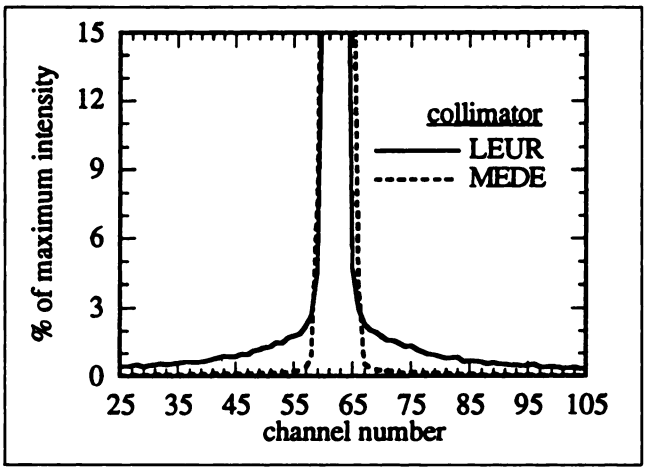

FIGURE 6. Line-spread functions for low- and medium-energy collimators.

TABLE 1
Volume and Activity Measurements

True sphere volume (ml)	Sphere-to-bkg. concentration ratio	Volume		Activity	
		%error	%s.d.	%error	%s.d.
3.4	2.5	376	26.6	187	26.2
3.4	5	148	8.9	20.8	10.6
3.4	10	84.0	13.0	−10.8	8.10
12.0	2.5	4.08	24.8	−19.2	20.2
12.0	5	−4.92	7.12	−26.5	6.63
12.0	10	−3.38	4.36	−25.4	4.36
21.5	2.5	−2.31	21.5	−17.4	18.3
21.5	5	−1.68	7.55	−20.0	6.23
21.5	10	−1.26	8.75	−22.1	5.12

S:B ratios. The general trend observed in the table is a less accurate measurement with a smaller sphere size and a smaller S:B ratio. For the smallest sphere (3.4 ml), the volume was grossly overestimated at all S:B ratios. The activity measurement for the same sphere was also overestimated at the 2.5 S:B ratio, but within approximately 20% at the two greater ratios. For the two larger spheres, the volume measurement was within 5% accuracy for all S:B ratios with a %s.d. that tended to increase with smaller S:B ratio to a maximum of approximately 25%. The activity measurement for the two larger spheres was consistently underestimated by approximately 20%–25% with a % standard deviation similar as in the volume measurement.

The SPECT images from each of the three S:B ratios are shown in Figure 7. The selected slice was approximately through the center of the spheres. The images illustrate the noise level and the degree of difficulty in distinguishing the sphere from the background. In the 10 S:B ratio image, all three spheres are clearly detectable with boundaries relatively easily distinguishable from background. In the 5 S:B ratio image, all three spheres are also detectable although the boundary of the smallest sphere is obscured. In the 2.5 S:B ratio image, the smallest sphere cannot be detected, and the boundaries of the other two spheres are obscured. In spite of the difficulty in detecting the sphere, the semiautomatic quantitation method will still find a boundary within the loose ROI. This boundary, however, is due solely to image noise and produces the

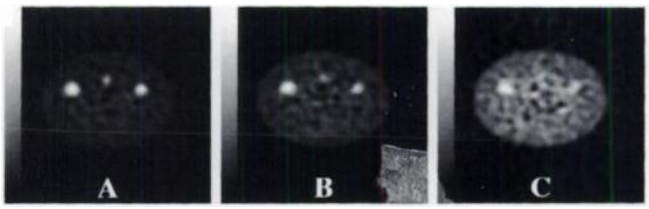

FIGURE 7. SPECT images through center of spheres for sphere-to-background ^{123}I concentration ratios of (A) 10, (B) 5 and (C) 2.5. Sphere size from left to right in each image is 21.5 ml, 3.4 ml and 12.0 ml.

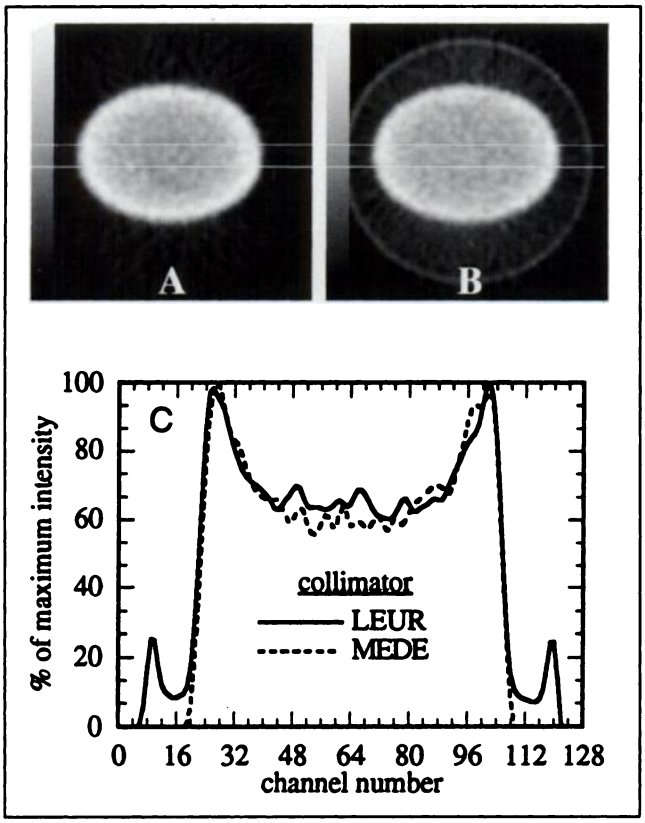

FIGURE 8. SPECT images of uniform cylinder with (A) medium-energy and (B) low-energy collimators and (C) profiles.

inaccurate quantitative results observed with the small sphere in Table 1.

DISCUSSION

The effect of penetration on SPECT quantitation with high-purity ^{123}I and low-energy, high-resolution collimators was found to be less than 5% for the particular source distribution in this study. While this effect should increase with the intensity of the surrounding activity, at this level it is relatively insignificant. Qualitatively, penetration effects can be observed in the SPECT image as a ring along the edge of the field of view. In Figure 7, this artifact becomes more prominent in lower S:B ratio images and is clearly seen in Figure 8 which shows reconstructed images (no attenuation compensation) and profiles through a uniform region of the cylinder at relatively high count density for both the LEUR and MEDE collimators.

This artifact has been noted previously (*5*) and is consistent with the planar line-spread function shown in Figure 6 where the effects of penetration appear as broad, nearly flat tails. A source distribution that would create a nearly flat projection in the absence of penetration is a ring located near the edge of the field of view in a transaxial slice. In spite of this noticeable artifact, the results of the quantitative study suggest that penetration effects in the SPECT image are primarily confined to the outer edge.

While the results of this study on the effect of ^{123}I penetration with low-energy collimators appear to contradict the suggestion from a previous investigation (*5*) that low-energy collimators are unsuitable for ^{123}I SPECT quantitation, there are differences between these two studies worth noting. The low-energy, high-resolution collimators used in the two studies are different which could result in different penetration effects. The LEUR collimators used in the present study had an approximately 50% longer hole length, 25% smaller hole diameter and the same septal thickness as the low-energy, high-resolution collimator used in the previous study. In general, one should expect variability in hole geometry and performance characteristics for different manufacturers' collimators in spite of a similar collimator classification. The method of ^{123}I production was also different in the two studies, and this could impact the relative degree of penetration due to different levels of contamination from other isotopes of iodine.

The gradient method implemented in this study for tumor-boundary detection differs from a previous method (*3*) in that the gradient calculation is only along radial lines emanating from the tumor center. This results in an efficient and practical quantitation method. In this study, the total processing time to extract the volume and activity measurements once the loose ROI has been specified in the SPECT image was found to be less than 2 sec (SPARCstation 2, Sun Microsystems, Inc., Mountain View, CA). One disadvantage to this approach is that errors in the estimated tumor boundary might be expected for tumors with convoluted shapes. However, tumors often encountered in SPECT Mab imaging, particularly primary and metastatic lung tumors and metastases to the liver and colon, tend not to appear convoluted but somewhat round in shape. This is due in part to the coarse spatial resolution relative to the tumor size. Another disadvantage is that for larger tumor sizes, eight radial gradients may be insufficient and result in quantitative errors. For these cases the method can be readily extended to include a greater number of radial gradients.

The quantitative ^{123}I SPECT method applied to the two largest spheres in this study accurately measured the volume but consistently underestimated the activity. The fact that the reconstructed activity concentration in the broad, background region of the phantom was within 10% of the planar measurement of a syringe containing background solution, points to spatial resolution effects as the primary cause of the underestimated sphere activity. A portion of the sphere's activity is reconstructed outside the object boundary. Greater resolution can be achieved by modifying the restoration filter but only at a cost of greater image noise. The effect of the filter on quantitative accuracy and precision requires further study. The fact that the activity was so consistently underestimated suggests that a more accurate result could be achieved by simple calibration of the activity measurement.

The sphere size and sphere-to-background ^{123}I concen-

tration ratios were selected to probe the limits of quantitative ^{123}I SPECT for this count density level. The results of this study show that for objects equal to or larger than 12 ml, accurate volume and activity measurements are possible for concentration ratios as low as 2.5. However, volume measurement of objects as small as 3.4 ml is impossible by these methods and activity measurement requires a concentration ratio greater than 5. For larger objects than investigated in this study, one could reasonably expect accuracy equal to or better than the largest object considered here (21.5 ml).

While the effect of count density was not investigated in this study, the count density was selected to be representative of clinical Mab imaging. In a study that gave two patients ^{123}I-labeled anti-CEA Mabs, 5-g resected carcinoma tumors contained ^{123}I activity concentrations of 0.0385 MBq/g and 0.235 MBq/g (*15*) which compares favorably with the 0.044 MBq/g-sphere activity concentration used in this study. For count densities lower than those studied here, we would expect an increase in the minimum object size and uptake ratio necessary for quantitatively accurate volume and activity measurement. The worsening of quantitative accuracy with decreasing count density has been described previously (*16*). If, however, the reduced count density comes with an increase in spatial resolution (e.g., as the result of using higher-resolution collimation), the effect on quantitative accuracy is difficult to predict (*17*).

The Chang attenuation compensation method based on a uniform attenuation map results in quantitative errors in objects having substantially nonuniform density such as those found in the human thoracic region. Several studies, however, have shown that SPECT quantitative accuracy can be greatly improved for nonuniformly dense objects by modifying the Chang method to incorporate a nonuniform attenuation map (*18–20*). Therefore we would expect comparable performance of the semiautomatic quantitative technique for nonuniform density objects if the appropriate attenuation compensation methods are applied.

ACKNOWLEDGMENTS

This work was supported by Department of Energy grant DE-FG05-89ER60894 and in part by PHS grant CA 33541.

REFERENCES

1. Hoffman EJ, Huang SC, Phelps ME. Quantitation in positron emission computed tomography: 1. effect of object size. *J Comput Assist Tomog* 1979;3:299–308.
2. King MA, Long DT, Brill AB. SPECT volume quantitation: influence of spatial resolution, source size and shape, and voxel size. *Med Phys* 1991; 18:1016–1024.
3. Long DT, King MA, Sheehan J. Comparative evaluation of image segmentation methods for volume quantitation in SPECT. *Med Phys* 1992;19:483–489.
4. Browne E, Dairiki JM, Doebler RE. In: Lederer CM, Shirley VS, eds. *Table of isotopes*. New York: Wiley and Sons; 1978:597.
5. Macey DJ, DeNardo GL, DeNardo SJ, Hines HH. Comparison of low- and medium-energy collimators for SPECT imaging with iodine-123-labeled antibodies. *J Nucl Med* 1986;27:1467–1474.
6. Bolmsjo M, Persson B, Strand S. Imaging ^{123}I with a scintillation camera. A study of detection performance and quality factor concepts. *Phys Med Biol* 1977;22:266–277.
7. McKeighen R, Muehllehner G, Mayer R. Gamma camera collimator considerations for imaging ^{123}I. *J Nucl Med* 1974;15:328–331.
8. Coleman RE, Greer KL, Drayer BP, Albright RE, Petry NA, Jaszczak RJ. Collimation for ^{123}I imaging with SPECT. In: Esser PD, ed. *Emission computed tomography—current trends*. New York: Society of Nuclear Medicine; 1983:135–145.
9. Chang LT. A method for attenuation correction in radionuclide computed tomography. *IEEE Trans Nucl Sci* 1978;25:638–643.
10. Hubbell JH. Photon cross sections, attenuation coefficients and energy absorption coefficients from 10 keV to 100 GeV. In: *National standards reference data series*, volume 29. Washington, DC: National Bureau of Standards; 1969:64.
11. Jaszczak RJ, Greer KL, Floyd CE, Harris CC, Coleman RE. Improved SPECT quantification using compensation for scattered photons. *J Nucl Med* 1984;25:893–900.
12. Metz CE, Beck RN. Quantitative effects of stationary linear image processing on noise and resolution of structure in radionuclide images. *J Nucl Med* 1974;15:164–170.
13. King MA, Schwinger RB, Penny BC, Dohertry P, Bianco JA. Digital restoration of indium-111 and iodine-123 SPECT images with optimized Metz filters. *J Nucl Med* 1986;27:1327–1336.
14. Budinger TF, Derenzo SE, Greenburg WL, Gullberg GT, Huseman RH. Quantitative potentials of dynamic emission computed tomography. *J Nucl Med* 1978;19:309–315.
15. Bischof-Delaloye A, Delaloye B, Buchegger F. Clinical value of immunoscintigraphy in colorectal carcinoma patients: a prospective study. *J Nucl Med* 1989;30:1646–1656.
16. Zanzonico PB, Bigler RE, Sgouros G, Strauss A. Quantitative SPECT in radiation dosimetry. *Semin Nucl Med* 1989;19:47–61.
17. Muehllehner G. Effect of resolution improvement on required count density in ECT imaging: a computer simulation. *Phys Med Biol* 1985;30:163–173.
18. Manglos SH, Jaszczak RJ, Floyd CE, Hahn LH, Greer KL, Coleman RE. Nonisotropic attenuation in SPECT: phantom test of quantitative effects and compensation techniques. *J Nucl Med* 1987;28:1584–1591.
19. Tsui BMW, Gullberg GT, Edgerton ER, et al. Correction of nonuniform attenuation in cardiac SPECT imaging. *J Nucl Med* 1989;30:497–507.
20. Gilland DR, Jaszczak RJ, Greer KL, Coleman RE. Quantitative SPECT reconstruction of iodine-123 data. *J Nucl Med* 1991;32:527–533.